

SUPPLEMENTARY INFORMATION

A dynamic core in human NQO1 controls the functional and stability effects of ligand binding and their communication across the enzyme dimer

Pavla Vankova, Eduardo Salido, David J. Timson, Petr Man and Angel L. Pey

Includes Figures S1-S11 and Tables S1-S2.

Figure S1. Purity and activity of the NQO1 protein. A) SDS-PAGE analysis (12 % acrylamide) of NQO1 protein purified upon expression in *E. coli*. Different gels show purified NQO1 protein (6-8 µg) as holo- and apo-proteins, respectively. Gels were stained with Coomassie® Brilliant blue R250 (Sigma-Aldrich). B) Enzyme kinetic analysis of holo-NQO1 in the presence of a fixed DCPIP concentration (20 µM) and variable concentrations of NADH. Prior to the assay, 1 nM holo-NQO1 was incubated in K-HEPES 50 mM pH 7.4 with NADH for 5 min at 25°C and the reaction triggered by adding DCPIP. Blanks in the absence of enzyme were also measured and subtracted. The specific activity was determined spectrophotometrically essentially as described [1]. Each point represents the average of two replicates. Data were collected in three independent experimental series. The line is a fit to the Michaelis-Menten equation providing values of k_{cat} and $K_{M(NADH)}$ of $50 \pm 4 \text{ s}^{-1}$ and $540 \pm 90 \mu\text{M}$, respectively.

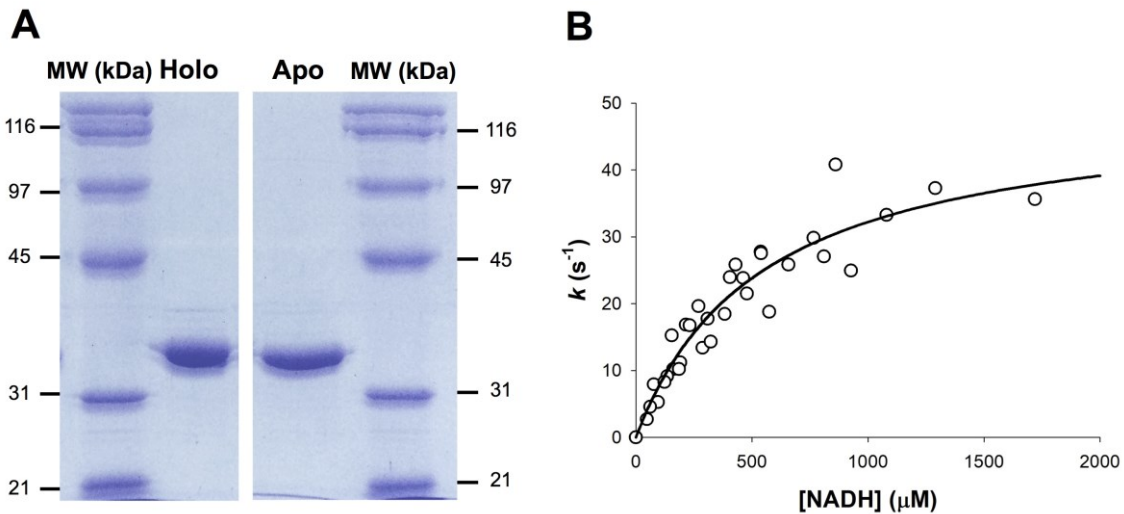


Figure S2. Verification of the NQO1 protein by high resolution mass spectrometry. NQO1 was offline desalted on a Protein OptiTrap (Optimize Technologies,). Then 5 μ M sample was directly infused into an ESI source of 15T FT-ICR MS (solariX XR, Bruker Daltonics) and the spectra were recorded in a broad band mode with 2M data points. Spectrum shows the entire charge state envelope (detected charges 19+ to 48+) and inset demonstrates the high resolving power and isotopic pattern for charge state 32+. Spectrum was deconvoluted using the SNAP algorithm (DataAnalysis 5.0). Calculated monoisotopic mass and the experimental deconvoluted values are shown together with the error in ppm. The precise mass exactly fits to the sequence of the construct (shown below the spectrum) without the N-terminal methionine (shown in grey). Grey highlight shows the His-tag sequence. This is also indicated by the negative (non-native) numbering.

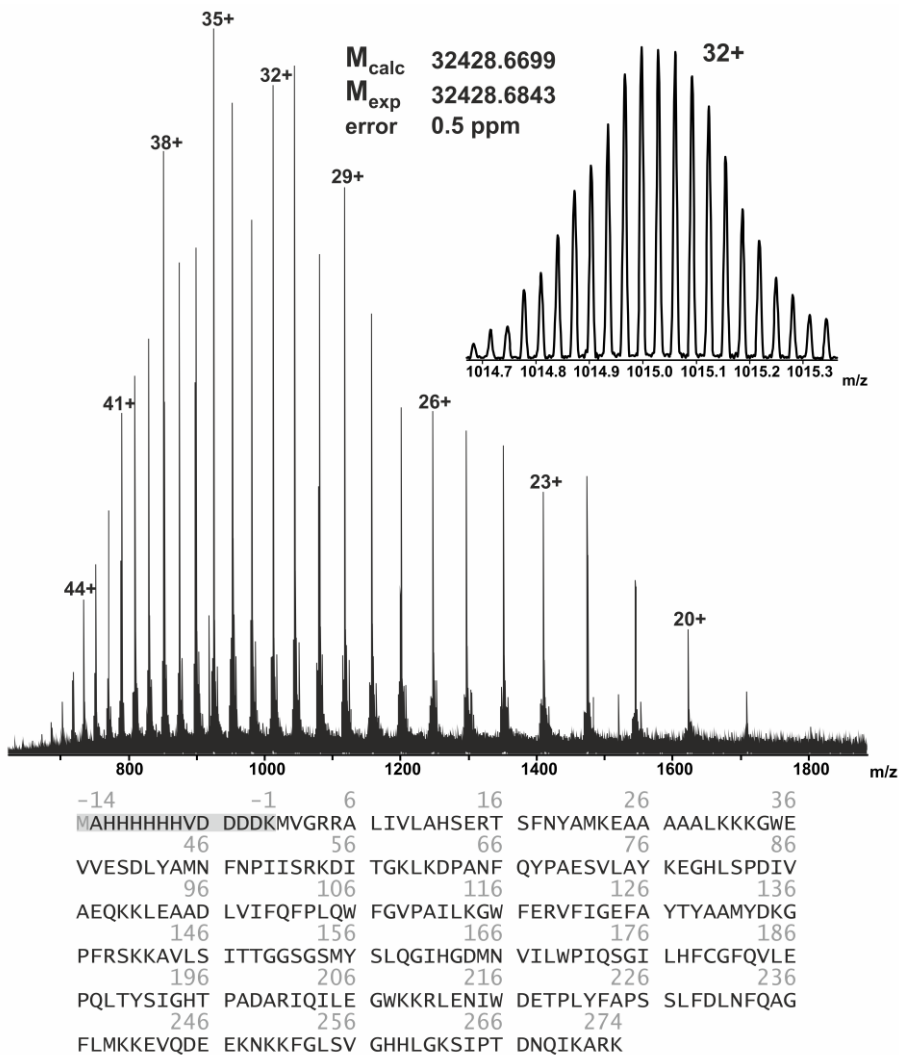


Figure S3. NQO1 dimeric state confirmed by mass spectrometry. NQO1_{apo} (A) and NQO1_{holo} (B) were transferred into 100 mM ammonium acetate pH 7.5 by Zeba spin (Thermo Fisher) desalting columns. Protein solution was transferred into a home-made quartz nESI emitter that was mounted to an nESI source of Synapt G2Si (Waters). Spray voltage was kept at 0.7 kV. Temperature was 20 °C, sampling cone and source offset were 50 V and 20 V, respectively. Trap collisional cooling (CE) of 80 V was required to achieve better S/N and resolution. The analyses proved that NQO1 forms stable dimer in both states. Charge states of individual peaks are shown. Dimeric protein state is indicated by two circles – open for NQO1_{apo} and closed for NQO1_{holo}.

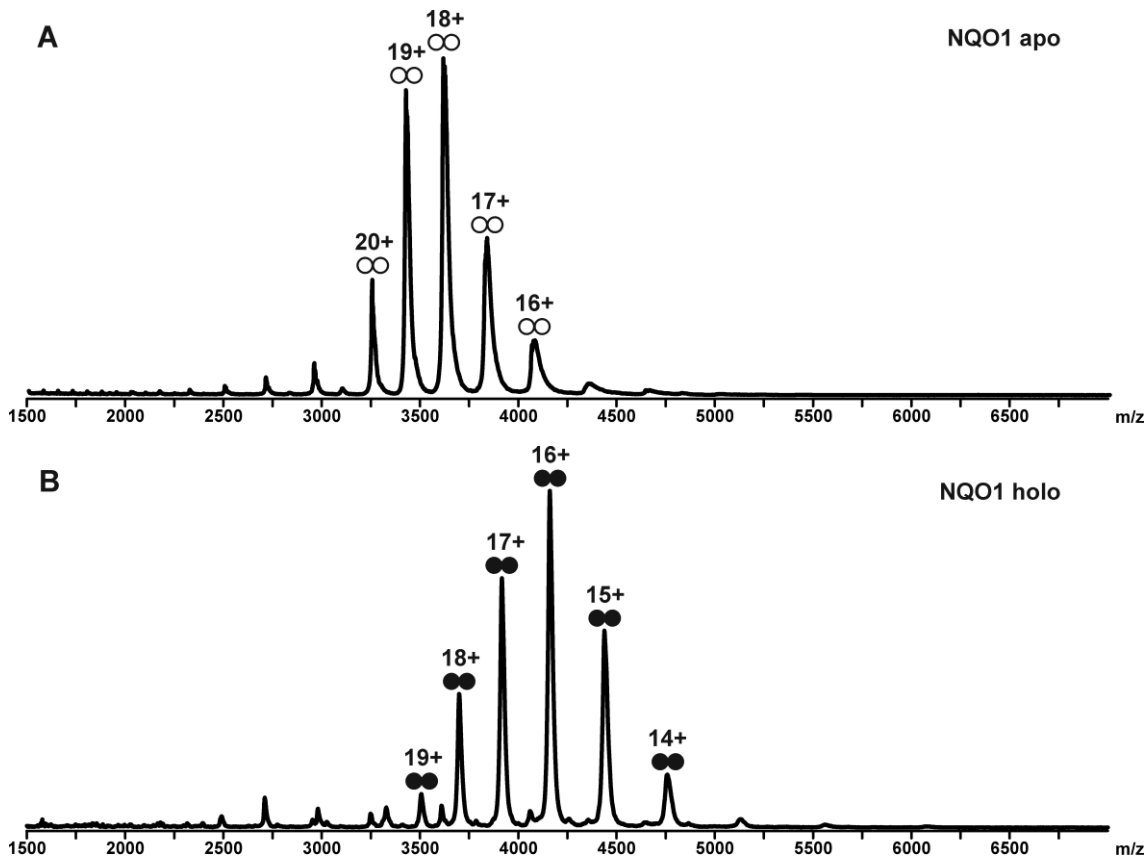


Figure S4. HDXMS mapping. NQO1 peptide map representing sequence coverage in the HDXMS study. Protein was digested online by a serial combination of Nepenthesin-2 and Pepsin. This yielded 140 peptides with the average peptide length 8.3 amino acids and redundancy score 4.05 covering nearly 99% of the sequence. Peptides were identified by LC-MS/MS analysis and MASCOT searching as described previously. Coverage is shown on the sequence of the construct with numbering reflecting native one. Secondary structure elements are shown as cylinders (alpha helices) and arrows (beta sheets). Numbering of loops is also indicated (L1-L10) above the sequence. The His-tag is highlighted as a grey box. Map was created using MSTools

(<http://peterslab.org/MSTools/DrawMap/DrawMap.php>). [2].

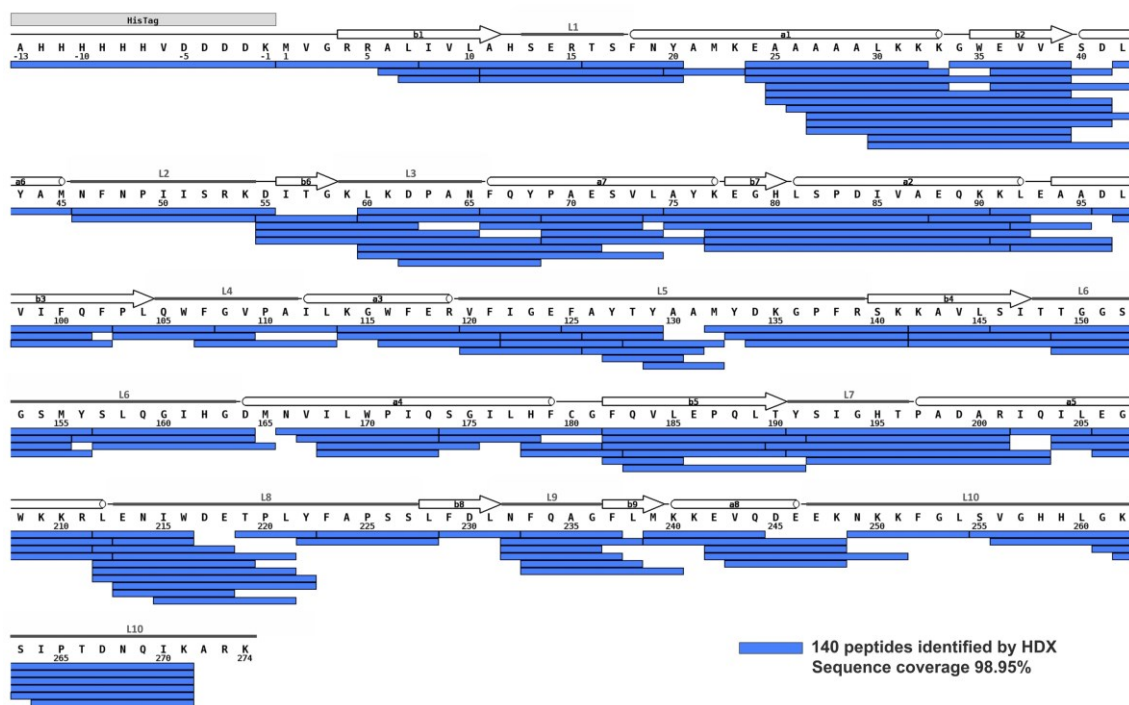


Figure S5. Representative examples of rare EX1/EX2 exchange profiles. The NQO1 protein showed predominantly EX2 exchange behavior in all ligation states as well as in the apo form. Exceptions were two regions covered by peptides 75-90, 77-90, 77-91, 77-92 and 249-254, 255-271, 256-271, 261-271, 262-271, 263-271, 264-271 where very small EX1 signatures were detected. Two representative examples are shown in this figure. A) Peptide 77-92 where top left graph shows peak width detected at 1% of the MS peak intensity as a function of time. Other three panels are showing isotopic envelopes of NQO1_{apo}, NQO1_{holo} and NQO1_{dic} at 300 s of exchange (position in the graph indicate this time point). B) peptide 255-271, peak width is again in the top left part of the panel and the other three panels show mass spectra of NQO1_{apo}, NQO1_{holo} and NQO1_{dic} at 10 s of exchange (position in the graph indicate this time point).

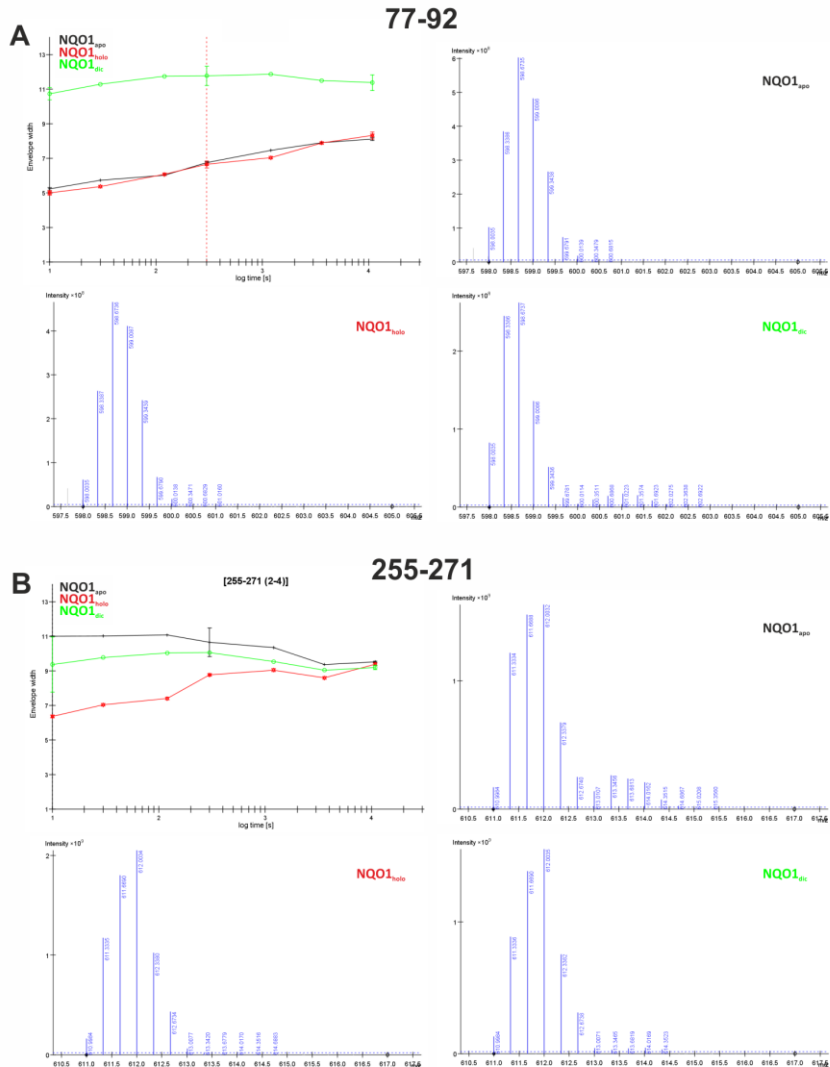


Figure S6 (1 of 3). HDX kinetics for NQO1 segments (spanning residues 1-95) of NQO1 upon FAD and dicoumarol binding. Plots show percentage of deuteration as a function of time. Segment limits are shown in each graph. Kinetic analysis can be found in Table S1.

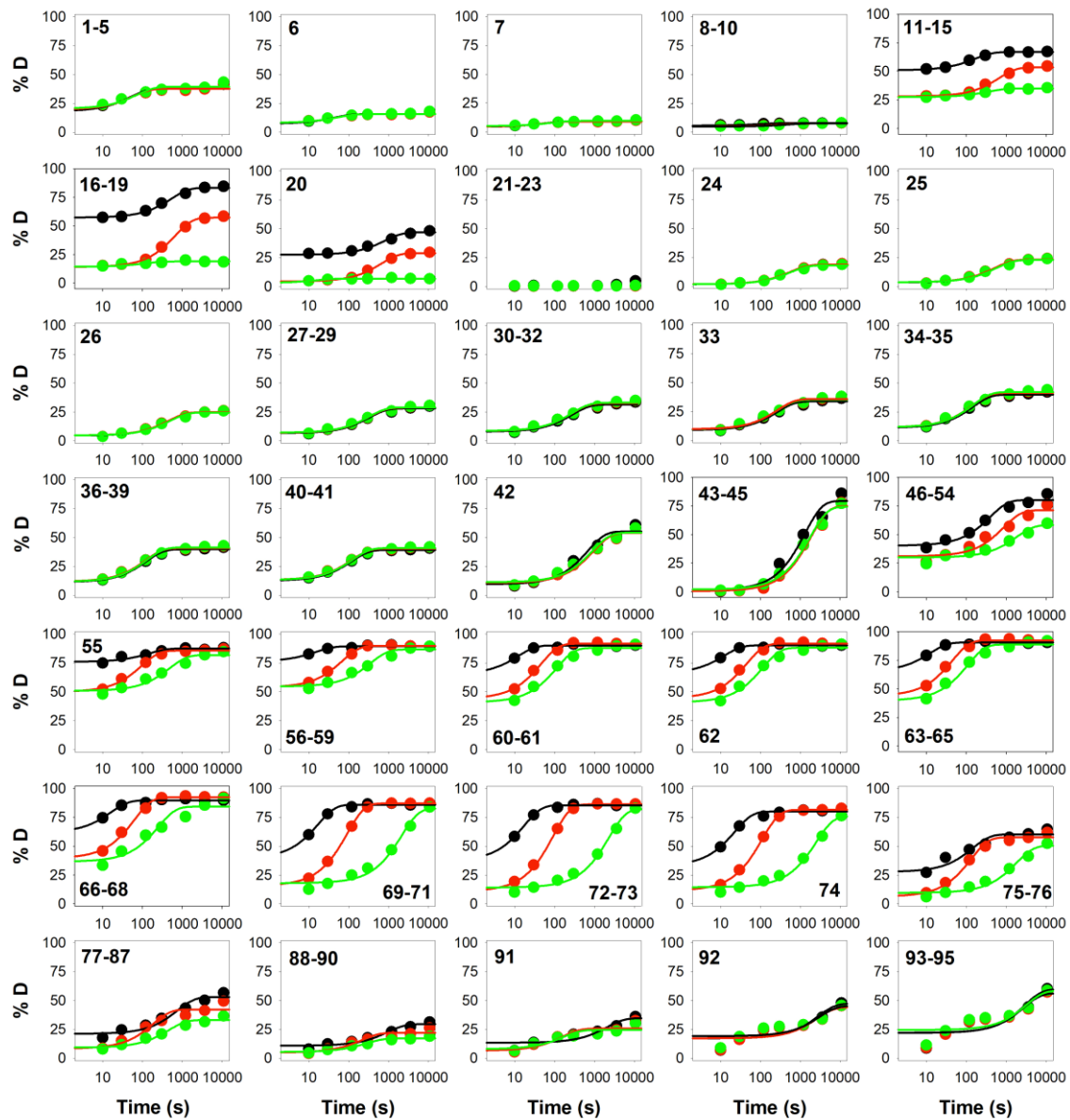


Figure S6 (2 of 3). HDX kinetics for NQO1 segments (spanning residues 96-181) of NQO1 upon FAD and dicoumarol binding. Plots show percentage of deuteration as a function of time. Segment limits are shown in each graph. Kinetic analysis can be found in Table S1.

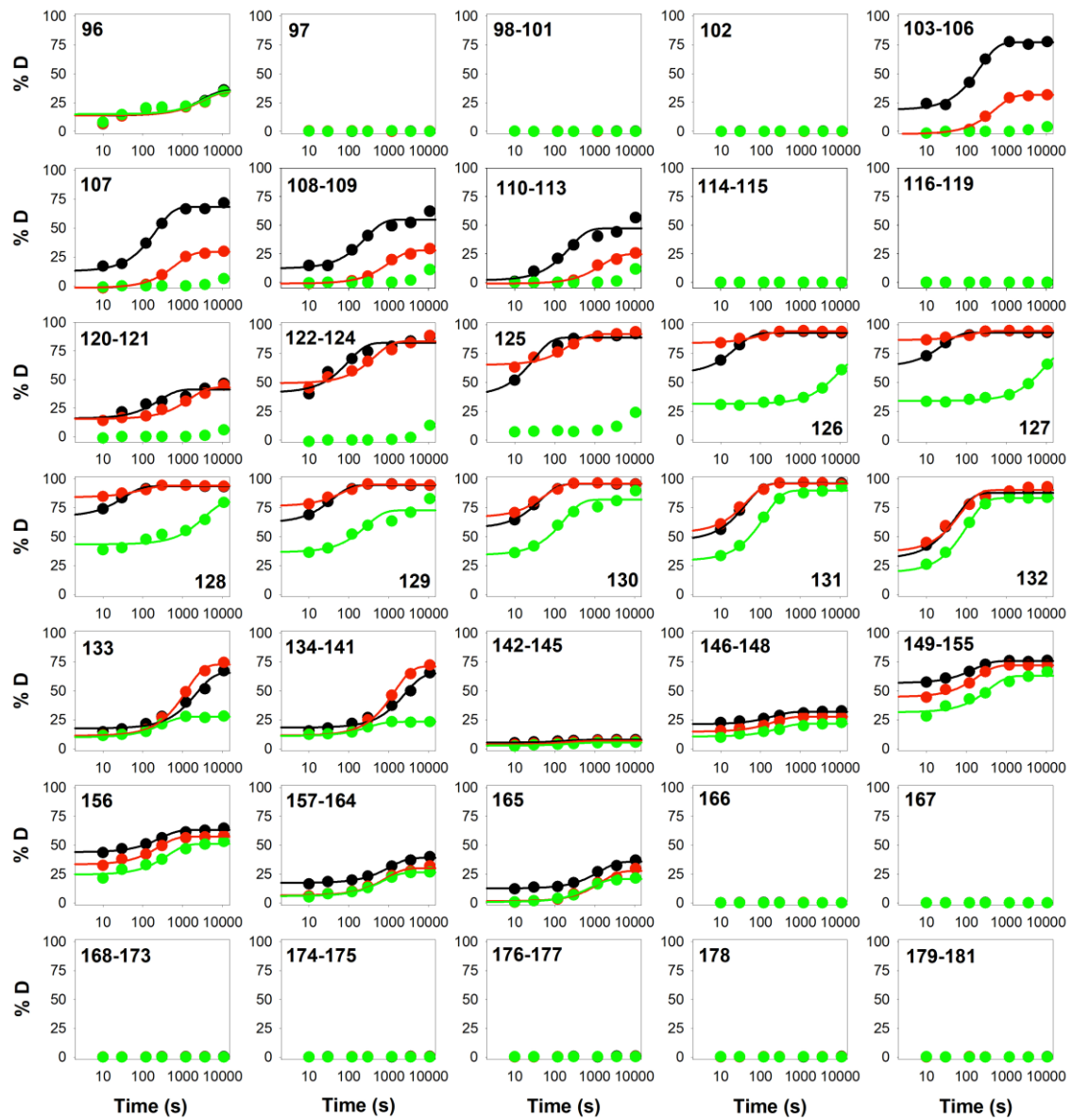


Figure S6 (3 of 3). HDX kinetics for NQO1 segments (spanning residues 182-271) of NQO1 upon FAD and dicoumarol binding. Plots show percentage of deuteration as a function of time. Segment limits are shown in each graph. Kinetic analysis can be found in Table S1.

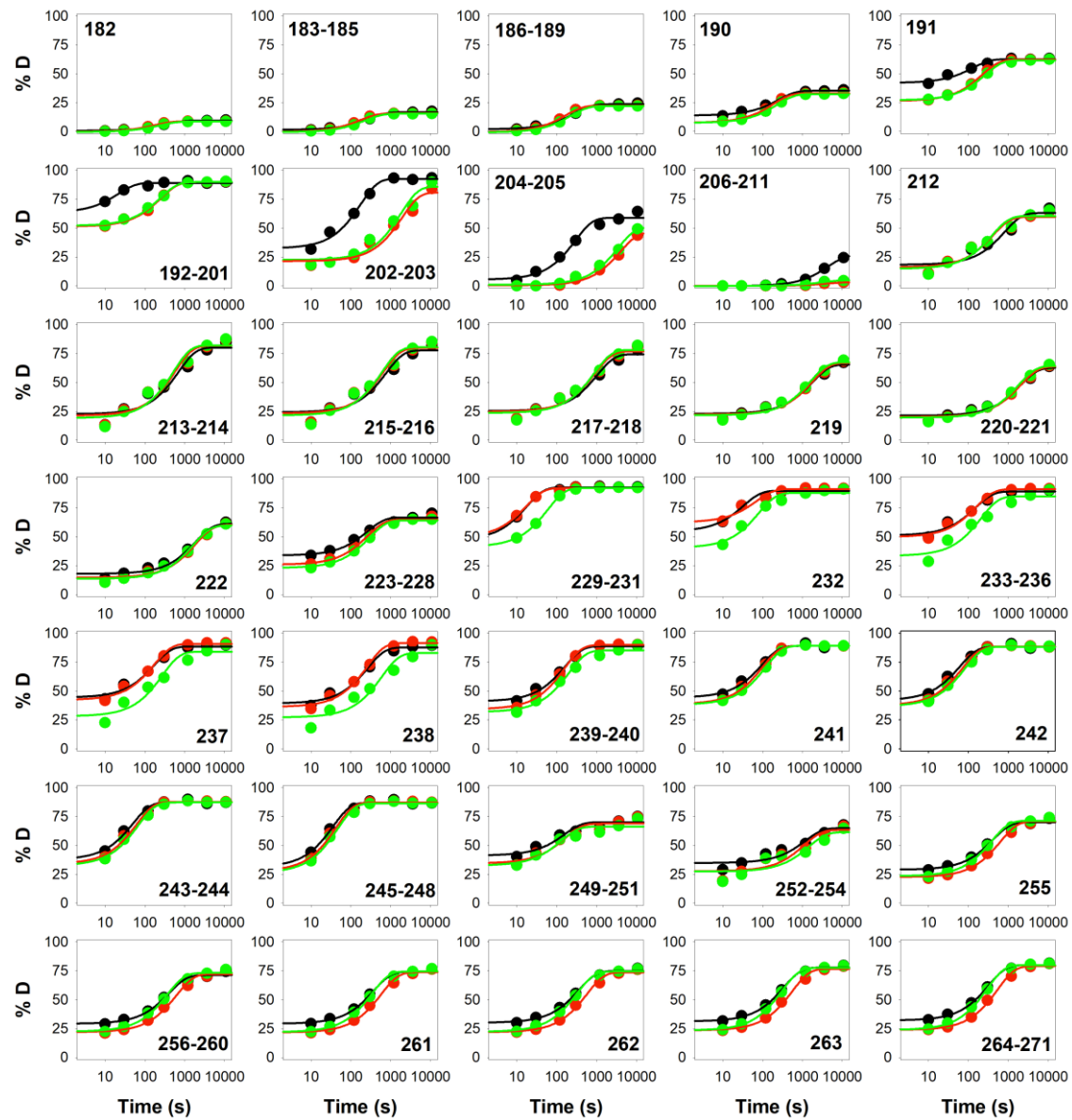


Figure S7. HDX kinetics for 39 non-overlapping and non-redundant peptides of NQO1 upon FAD and dicoumarol binding. Plots show percentage of deuteration as a function of time. Peptide limits are shown in each graph. These analyses are meant to be compared with those displayed in Figures S6. Kinetic analyses can be found in Table S2.

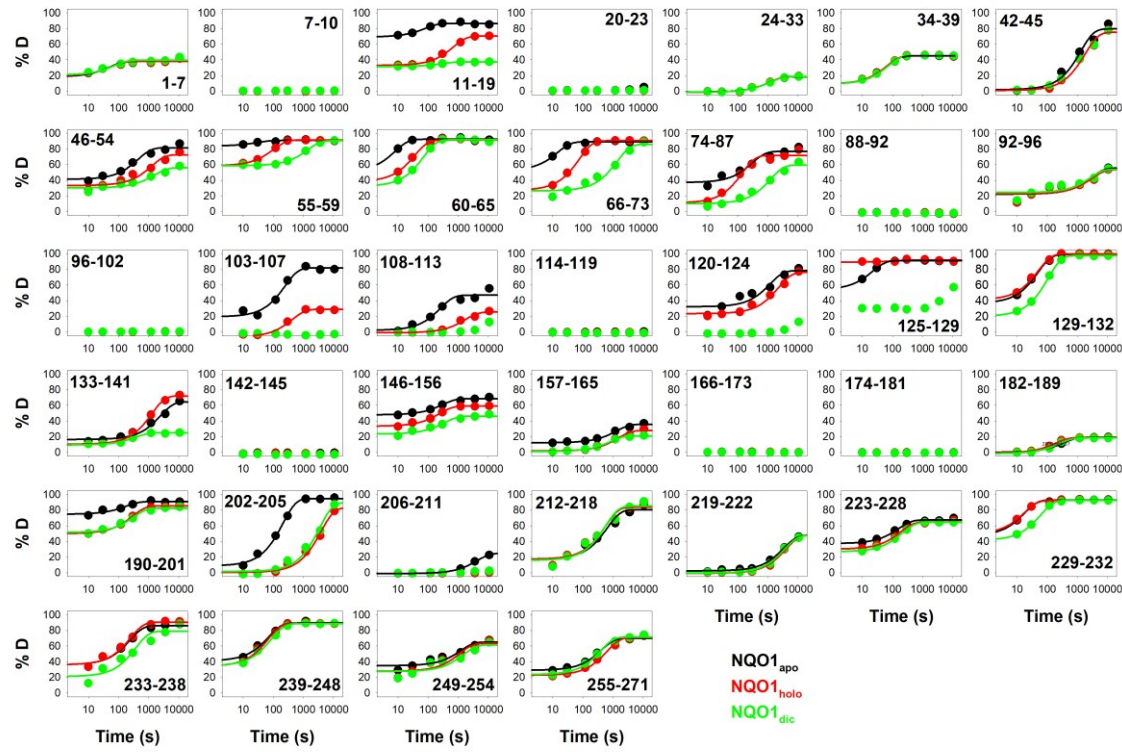


Figure S8. Non-exchanging peptides define a minimal stable core in NQO1_{apo}.

A) Plot of the % SASA for individual residues (considering backbone and side-chain) calculated as indicated Figure 3. Secondary structure elements are depicted according to [3]; B) Structural representation of non-exchanging residues (using PDB 2F10; [4]). The left panel shows a surface representation highlighting the burial of the minimal and stable core. The middle panel shows segments belonging to this core plotted onto secondary structures. The right panel shows that the core may contribute to the stable folding of the individual monomers as well as their assembly into the dimer, with only some stable contacts with the FAD (in orange ball representation) and the dicoumarol (in yellow ball representation). Note that this analysis for the 39 experimental peptides (Table S2) only shows small differences (a longer α 1 helix and a *new* non-exchanging short segment in helix α 2) vs. those carried out with NQO1 segments (Table S1 and Figure 3).

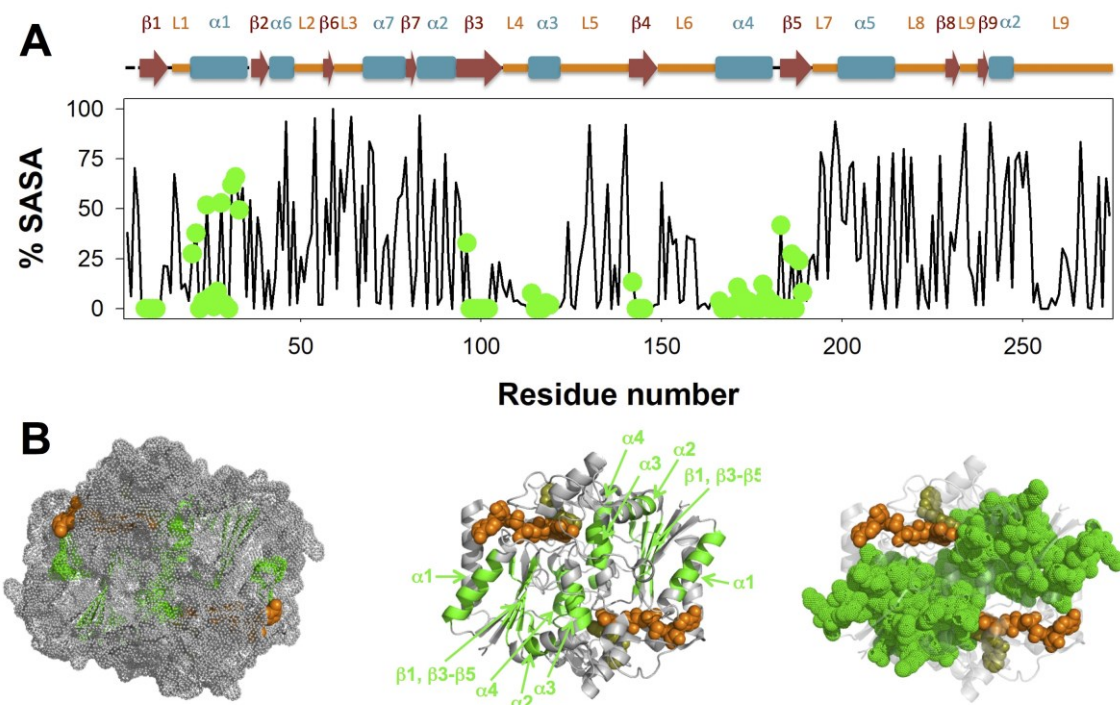


Figure S9. Specific HDX kinetics for 39 peptides of NQO1_{apo}. A) Plots of the amplitudes for the burst- and slow-phase in HDX for peptides (upper panel) and rate constant for the slow phase (lower panel) for peptides with at least 20% D after 3 h. The elements of secondary structure along the protein sequence are also indicated. Note that this analysis for the 39 experimental peptides (Table S2) show little differences when compared with those carried out with NQO1 segments (Table S1 and Figure 4).

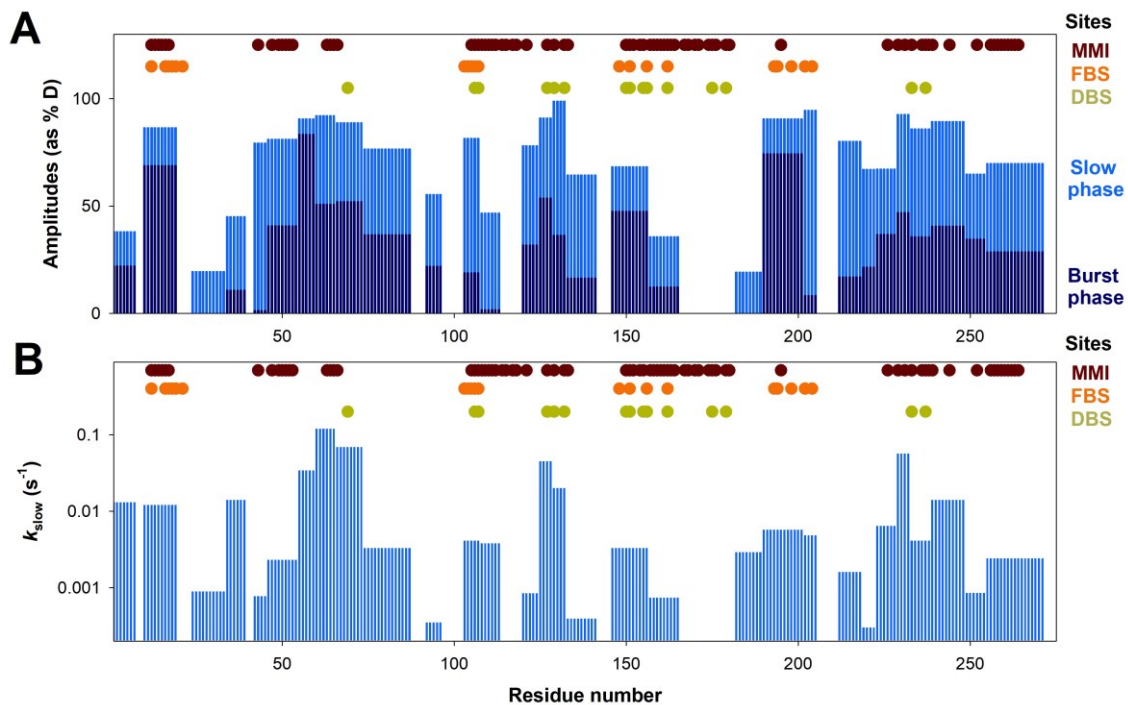


Figure S10. Changes in HDX kinetics for 39 peptides of NQO1 upon binding FAD and dicoumarol as changes in %D_{av} ($\Delta\%$ D_{av}). A) $\Delta\%$ D_{av} for peptides upon binding FAD (NQO1_{holo}) and dicoumarol (NQO1_{dic}) using of NQO1_{apo} as a reference (see Figure 7 for details). B) Representation of ($\Delta\%$ D_{av}) onto the structure of NQO1 (using PDB code 2F10). The upper row shows the results for $\Delta\%$ D_{av} for NQO1_{holo} and lower row represents NQO1_{dic}. Different panels in each row show results for residues involved in the FBS, DBS or MMI. Note that this analysis for 39 experimental peptides (Table S2) shows little differences with those data carried out with NQO1 segments (Table S1 and Figure 7).

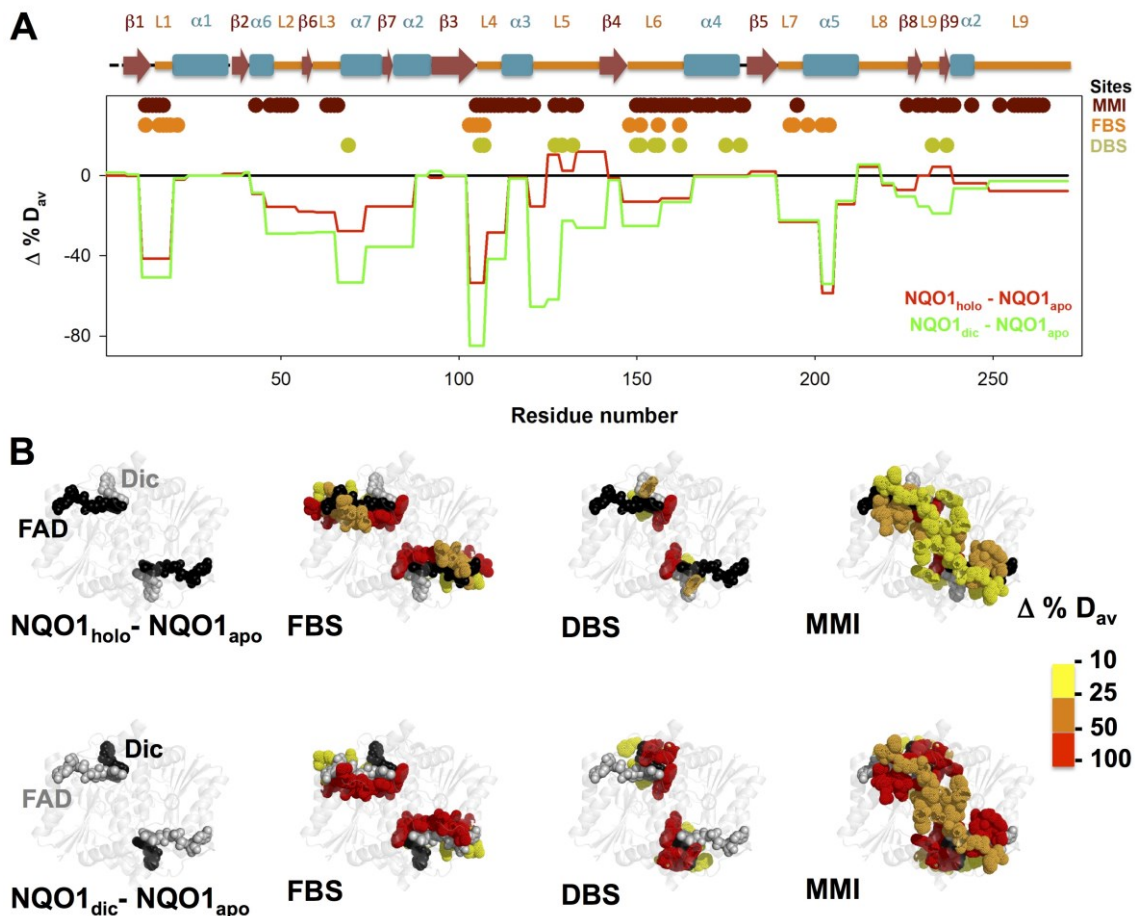
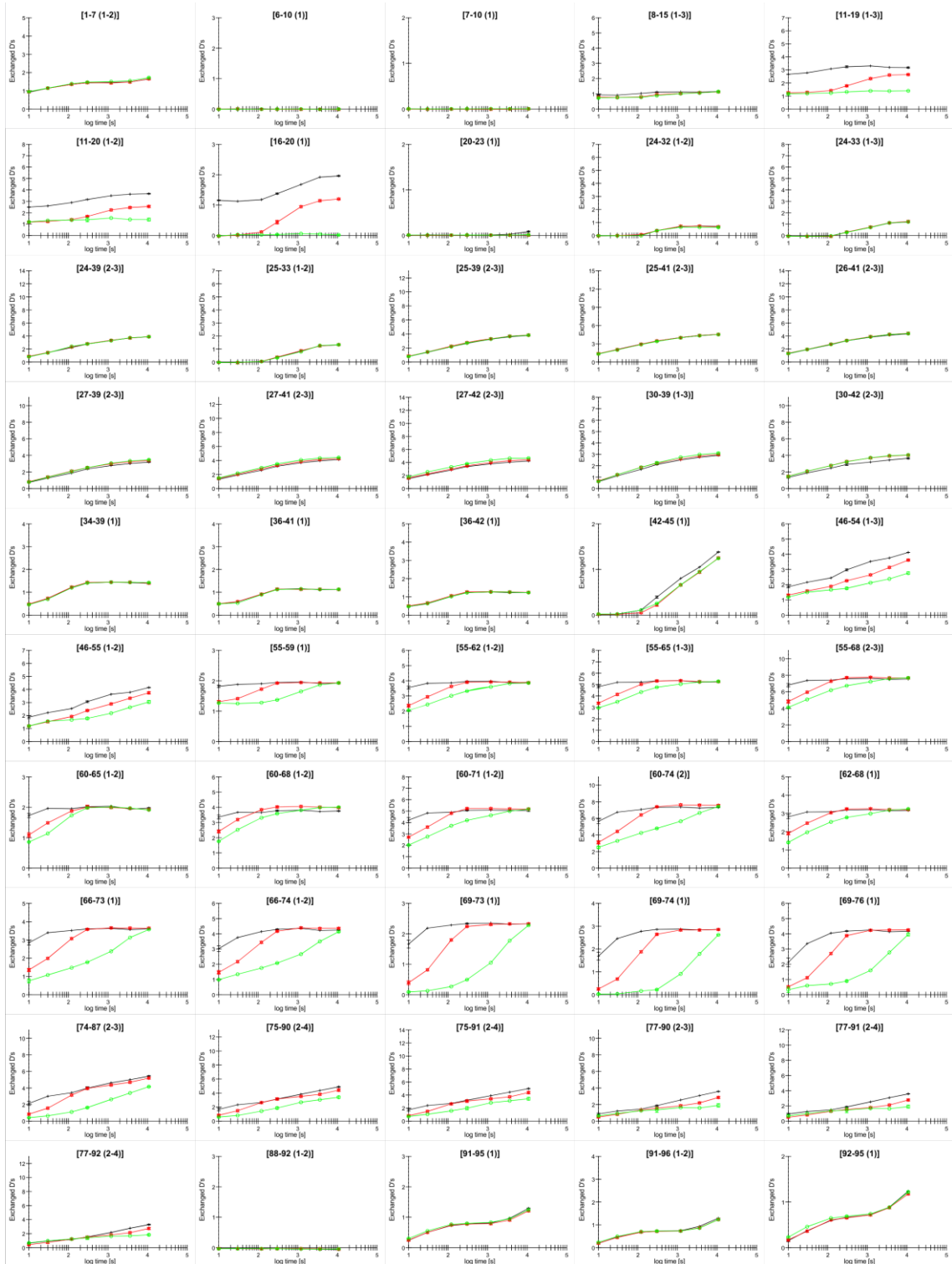
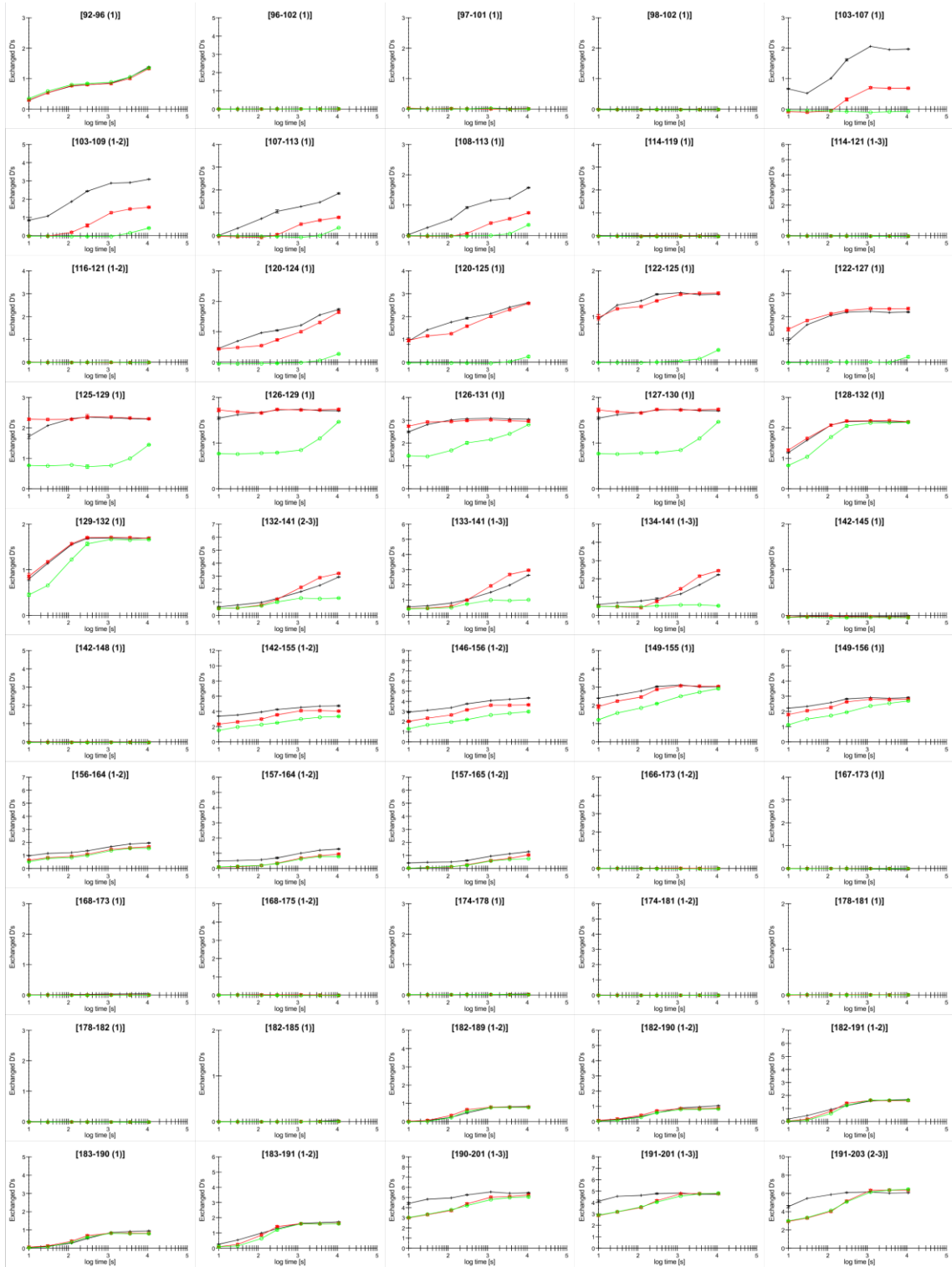


Figure S11 (three pages). HDX kinetics for all peptides detected in HDXMS experiments. Each peptide is represented by one deuterium uptake plot where number of deuterons is plotted as a function of time. Black stands for NQO1_{apo}, red for NQO1_{holo} and green for NQO1_{dic}. Times points followed during experiment were 10 s, 30 s, 2 min, 5 min, 20 min, 1 h and 3 h. Labeling and analysis at 10 s, 5 min and 3 h was replicated and the data are shown as average values with standard deviation (error bars at these points). Peptide limits are shown at the top of each graph together with the range or charge states that were detected for the peptide.





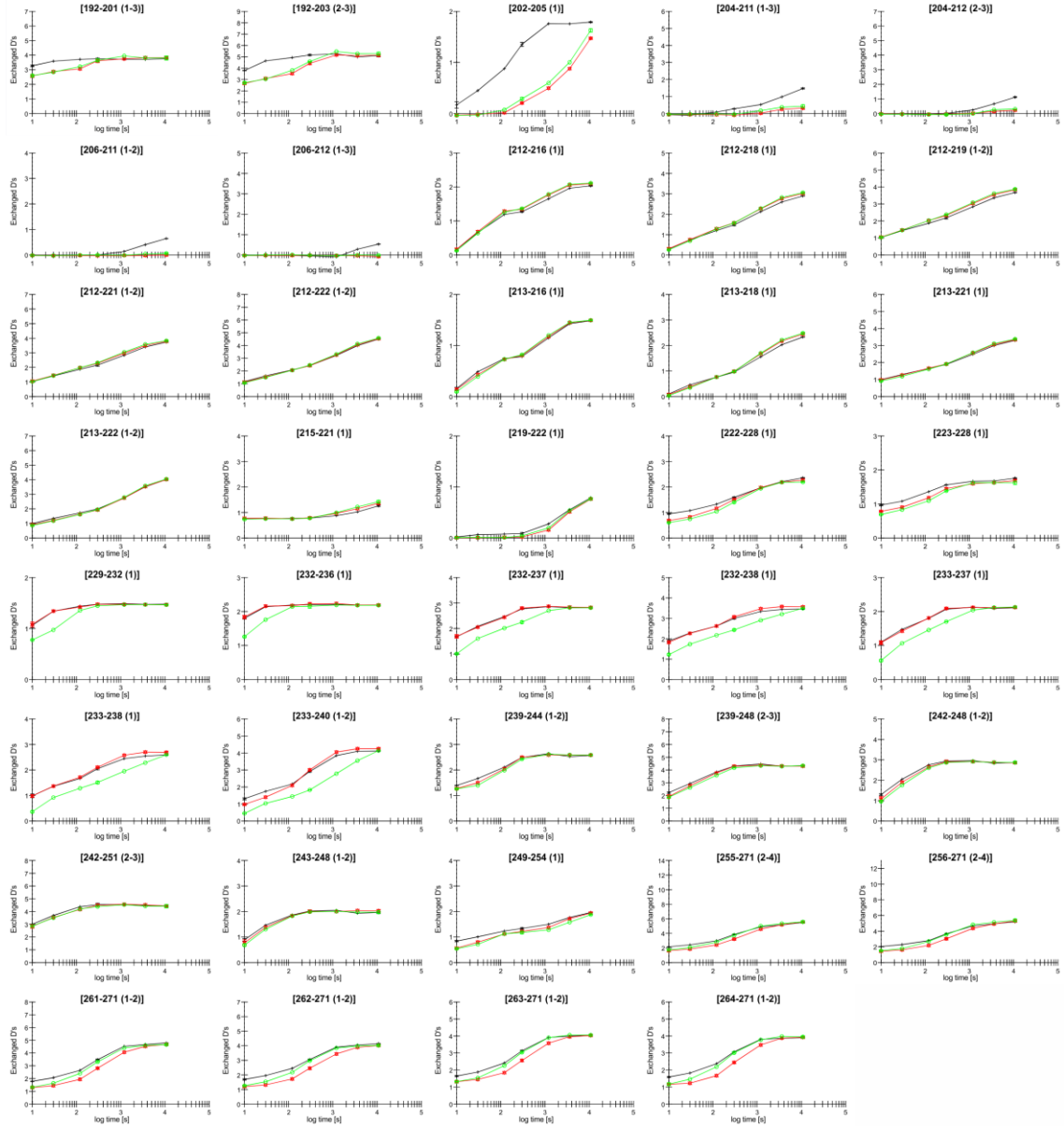


Table S1. Kinetic parameters for fitting of HDX kinetics to a three-parameter exponential function for NQO1 segments. SLNE indicates slow, little or no exchange.

Segment	NQO1 protein	Aburst (%D)	A _{slow} (%D)	k _{slow} (s ⁻¹)	R ²
1-5	NQO1 _{apo}	22.3±2.7	15.8±2.8	1.2±0.6 ·10 ⁻²	0.914
	NQO1 _{holo}	23.0±2.8	15.0±2.8	1.2±0.6 ·10 ⁻²	0.898
	NQO1 _{dic}	23.5±2.6	16.2±2.7	1.0±0.5 ·10 ⁻²	0.912
6	NQO1 _{apo}	8.8±1.3	7.0±1.3	1.5±0.8 ·10 ⁻²	0.916
	NQO1 _{holo}	9.6±1.2	6.3±1.2	1.2±0.7 ·10 ⁻²	0.893
	NQO1 _{dic}	9.5±1.2	7.0±1.2	1.1±0.5 ·10 ⁻²	0.912
7	NQO1 _{apo}	5.2±0.7	4.0±0.7	1.4±0.7 ·10 ⁻²	0.915
	NQO1 _{holo}	5.5±0.7	3.7±0.7	1.2±0.7 ·10 ⁻²	0.893
	NQO1 _{dic}	5.6±0.6	4.1±0.6	1.0±0.4 ·10 ⁻²	0.921
8-10	NQO1 _{apo}	6.1±0.1	1.7±0.1	7.7±1.9 ·10 ⁻³	0.973
	NQO1 _{holo}	5.3±0.2	2.3±0.2	1.9±0.7 ·10 ⁻³	0.957
	NQO1 _{dic}	5.0±0.2	2.7±0.3	1.6±0.5 ·10 ⁻³	0.966
11-15	NQO1 _{apo}	51.0±0.3	15.9±0.4	6.0±0.4 ·10 ⁻³	0.998
	NQO1 _{holo}	28.1±0.7	25.5±1.0	1.5±0.2 ·10 ⁻³	0.994
	NQO1 _{dic}	27.5±0.4	7.6±0.5	2.7±0.6 ·10 ⁻³	0.983
16-19	NQO1 _{apo}	57.4±1.0	26.0±1.3	1.9±0.3 ·10 ⁻³	0.990
	NQO1 _{holo}	14.6±0.8	42.8±1.1	1.5±0.1 ·10 ⁻³	0.997
	NQO1 _{dic}	15.4±0.7	3.6±0.8	5.2±3.2 ·10 ⁻³	0.845
20	NQO1 _{apo}	28.7±0.6	18.5±0.9	1.0±0.2 ·10 ⁻³	0.990
	NQO1 _{holo}	4.5±0.5	24.5±0.6	1.5±0.1 ·10 ⁻³	0.997
	NQO1 _{dic}	5.2±0.6	1.7±0.6	1.0±1.1 ·10 ⁻²	0.695
21-23	NQO1 _{apo}			SLNE	
	NQO1 _{holo}			SNLE	
	NQO1 _{dic}			SNLE	
24	NQO1 _{apo}	1.7±0.7	17.0±0.8	1.7±0.3 ·10 ⁻³	0.990

	NQO1 _{holo}	1.8±0.6	16.9±0.8	1.8±0.3 ·10 ⁻³	0.992
	NQO1 _{dic}	1.7±0.7	16.4±0.8	1.8±0.3 ·10 ⁻³	0.989
25	NQO1 _{apo}	3.7±1.0	19.5±1.3	1.9±0.4 ·10 ⁻³	0.983
	NQO1 _{holo}	3.7±1.0	19.5±1.3	1.9±0.4 ·10 ⁻³	0.984
	NQO1 _{dic}	3.8±1.0	19.2±1.3	1.8±0.4 ·10 ⁻³	0.982
26	NQO1 _{apo}	4.6±1.2	20.0±1.5	2.2±0.5 ·10 ⁻³	0.979
	NQO1 _{holo}	4.7±1.2	20.1±1.4	2.2±0.5 ·10 ⁻³	0.980
	NQO1 _{dic}	4.7±1.2	19.8±1.5	2.1±0.5 ·10 ⁻³	0.977
27-29	NQO1 _{apo}	6.9±1.5	21.2±1.8	2.9±0.5 ·10 ⁻³	0.974
	NQO1 _{holo}	7.3±1.5	21.5±1.8	3.0±0.7 ·10 ⁻³	0.975
	NQO1 _{dic}	7.4±1.5	21.6±1.9	2.9±0.7 ·10 ⁻³	0.973
30-32	NQO1 _{apo}	8.3±1.7	23.1±2.1	3.4±0.9 ·10 ⁻³	0.970
	NQO1 _{holo}	9.0±1.8	23.7±2.1	3.5±0.9 ·10 ⁻³	0.972
	NQO1 _{dic}	9.1±1.8	24.1±2.2	3.5±0.9 ·10 ⁻³	0.971
33	NQO1 _{apo}	9.5±2.0	24.4±2.4	3.5±1.0 ·10 ⁻³	0.965
	NQO1 _{holo}	10.3±2.1	25.7±2.5	3.5±1.0 ·10 ⁻³	0.964
	NQO1 _{dic}	10.4±2.1	25.7±2.3	3.5±1.0 ·10 ⁻³	0.963
34-35	NQO1 _{apo}	12.3±2.1	27.8±2.3	6.4±1.5 ·10 ⁻³	0.975
	NQO1 _{holo}	13.0±2.1	28.6±2.4	6.7±1.5 ·10 ⁻³	0.976
	NQO1 _{dic}	12.9±2.2	29.4±2.5	6.4±1.5 ·10 ⁻³	0.974
36-39	NQO1 _{apo}	12.5±1.5	27.4±1.6	7.5±1.2 ·10 ⁻³	0.988
	NQO1 _{holo}	13.1±1.5	27.9±1.7	7.9±1.3 ·10 ⁻³	0.987
	NQO1 _{dic}	12.9±1.6	28.6±1.7	7.3±1.2 ·10 ⁻³	0.988
40-41	NQO1 _{apo}	12.6 ±1.4	26.7±1.5	8.3±1.3 ·10 ⁻³	0.988
	NQO1 _{holo}	13.3±1.5	27.1±1.6	8.4±1.4 ·10 ⁻³	0.988
	NQO1 _{dic}	13.3±1.4	27.7±1.5	7.9±1.2 ·10 ⁻³	0.989
42	NQO1 _{apo}	9.5±3.4	45.7±4.6	1.4±0.5 ·10 ⁻³	0.961
	NQO1 _{holo}	10.8±2.6	43.3±3.8	1.0±0.3 ·10 ⁻³	0.971
	NQO1 _{dic}	11.3±2.7	42.9±3.9	1.1±0.3 ·10 ⁻³	0.969

43-45	NQO1 _{apo}	1.6 ± 3.6	77.8 ± 6.7	$7.7 \pm 1.8 \cdot 10^{-4}$	0.987
	NQO1 _{holo}	0.6 ± 2.7	74.4 ± 4.7	$5.4 \pm 1.1 \cdot 10^{-4}$	0.987
	NQO1 _{dic}	2.0 ± 2.3	72.2 ± 4.2	$5.7 \pm 1.0 \cdot 10^{-4}$	0.988
46-54	NQO1 _{apo}	40.4 ± 3.1	39.9 ± 3.8	$2.5 \pm 0.8 \cdot 10^{-3}$	0.966
	NQO1 _{holo}	31.1 ± 3.6	40.2 ± 5.1	$1.1 \pm 0.5 \cdot 10^{-3}$	0.940
	NQO1 _{dic}	30.0 ± 2.1	28.4 ± 3.9	$5.4 \pm 2.3 \cdot 10^{-4}$	0.939
55	NQO1 _{apo}	75.9 ± 1.5	11.6 ± 1.7	$6.7 \pm 2.7 \cdot 10^{-3}$	0.930
	NQO1 _{holo}	50.0 ± 1.7	35.7 ± 1.8	$1.0 \pm 0.1 \cdot 10^{-2}$	0.992
	NQO1 _{dic}	50.8 ± 2.7	31.0 ± 3.4	$2.1 \pm 0.8 \cdot 10^{-3}$	0.954
56-59	NQO1 _{apo}	76.3 ± 4.9	13.1 ± 4.8	$6.5 \pm 3.1 \cdot 10^{-2}$	0.898
	NQO1 _{holo}	53.8 ± 1.2	36.1 ± 1.2	$1.4 \pm 0.1 \cdot 10^{-2}$	0.997
	NQO1 _{dic}	54.5 ± 2.7	32.1 ± 3.2	$2.8 \pm 0.9 \cdot 10^{-3}$	0.963
60-61	NQO1 _{apo}	65.2 ± 8.8	24.9 ± 8.7	$8.1 \pm 3.2 \cdot 10^{-2}$	0.938
	NQO1 _{holo}	44.0 ± 2.8	47.7 ± 2.7	$2.2 \pm 0.3 \cdot 10^{-2}$	0.993
	NQO1 _{dic}	40.9 ± 3.6	47.1 ± 3.8	$8.7 \pm 2.0 \cdot 10^{-3}$	0.978
62	NQO1 _{apo}	66.0 ± 8.6	24.2 ± 8.5	$8.0 \pm 3.2 \cdot 10^{-2}$	0.938
	NQO1 _{holo}	44.4 ± 2.8	47.5 ± 2.8	$2.2 \pm 0.3 \cdot 10^{-2}$	0.993
	NQO1 _{dic}	40.9 ± 3.9	47.3 ± 4.1	$8.7 \pm 2.1 \cdot 10^{-3}$	0.974
63-65	NQO1 _{apo}	65.2 ± 8.9	25.4 ± 8.8	$8.0 \pm 3.2 \cdot 10^{-2}$	0.938
	NQO1 _{holo}	43.9 ± 2.9	48.8 ± 2.9	$2.2 \pm 0.3 \cdot 10^{-2}$	0.993
	NQO1 _{dic}	39.8 ± 4.0	49.1 ± 4.2	$9.2 \pm 2.2 \cdot 10^{-3}$	0.975
66-68	NQO1 _{apo}	61.8 ± 5.5	27.9 ± 5.5	$6.2 \pm 1.6 \cdot 10^{-2}$	0.966
	NQO1 _{holo}	39.5 ± 2.4	53.0 ± 2.4	$1.6 \pm 0.2 \cdot 10^{-2}$	0.995
	NQO1 _{dic}	36.6 ± 5.9	47.6 ± 6.9	$4.0 \pm 1.7 \cdot 10^{-3}$	0.926
69-71	NQO1 _{apo}	39.5 ± 4.6	46.4 ± 4.6	$5.8 \pm 0.8 \cdot 10^{-2}$	0.991
	NQO1 _{holo}	15.7 ± 1.0	71.3 ± 1.0	$1.1 \pm 0.1 \cdot 10^{-2}$	0.999
	NQO1 _{dic}	18.0 ± 2.5	64.7 ± 4.9	$4.7 \pm 1.0 \cdot 10^{-4}$	0.982
72-73	NQO1 _{apo}	37.2 ± 4.6	48.2 ± 4.5	$5.8 \pm 0.7 \cdot 10^{-2}$	0.991
	NQO1 _{holo}	11.0 ± 1.5	75.1 ± 1.5	$1.1 \pm 0.1 \cdot 10^{-2}$	0.998

	NQO1 _{dic}	14.2 ± 2.2	68.1 ± 4.5	$4.3 \pm 0.8 \cdot 10^{-4}$	0.968
74	NQO1 _{apo}	33.1 ± 6.7	46.9 ± 6.7	$4.3 \pm 1.0 \cdot 10^{-2}$	0.975
	NQO1 _{holo}	11.5 ± 1.2	69.9 ± 1.3	$9.1 \pm 0.5 \cdot 10^{-3}$	0.999
	NQO1 _{dic}	14.5 ± 2.0	61.5 ± 4.1	$4.0 \pm 0.8 \cdot 10^{-4}$	0.986
	NQO1 _{apo}	30.2 ± 4.3	30.3 ± 4.8	$5.9 \pm 2.6 \cdot 10^{-3}$	0.914
75-76	NQO1 _{holo}	7.2 ± 3.0	50.4 ± 3.2	$7.4 \pm 1.3 \cdot 10^{-3}$	0.985
	NQO1 _{dic}	9.9 ± 2.0	40.7 ± 3.7	$5.4 \pm 1.5 \cdot 10^{-4}$	0.975
	NQO1 _{apo}	22.2 ± 2.6	31.1 ± 3.7	$1.2 \pm 0.5 \cdot 10^{-3}$	0.946
77-87	NQO1 _{holo}	9.0 ± 4.4	33.4 ± 5.0	$5.2 \pm 2.2 \cdot 10^{-3}$	0.922
	NQO1 _{dic}	9.8 ± 2.1	23.5 ± 2.7	$2.0 \pm 0.8 \cdot 10^{-3}$	0.951
	NQO1 _{apo}	10.9 ± 1.5	18.7 ± 2.3	$1.0 \pm 0.4 \cdot 10^{-3}$	0.946
88-90	NQO1 _{holo}	5.0 ± 2.6	17.2 ± 3.0	$4.6 \pm 2.3 \cdot 10^{-3}$	0.894
	NQO1 _{dic}	5.4 ± 1.2	11.9 ± 1.4	$3.5 \pm 1.3 \cdot 10^{-3}$	0.948
	NQO1 _{apo}	13.5 ± 2.7	21.2 ± 5.3	$4.9 \pm 3.6 \cdot 10^{-4}$	0.831
91	NQO1 _{holo}	6.6 ± 4.5	19.2 ± 5.0	$6.3 \pm 4.5 \cdot 10^{-3}$	0.803
	NQO1 _{dic}	7.9 ± 3.8	16.6 ± 4.3	$6.0 \pm 4.3 \cdot 10^{-3}$	0.805
	NQO1 _{apo}	17.3 ± 3.9	30.0 ± 8.8	$3.6 \pm 3.0 \cdot 10^{-4}$	0.803
92	NQO1 _{holo}	17.4 ± 4.0	27.0 ± 8.6	$3.8 \pm 3.5 \cdot 10^{-4}$	0.769
	NQO1 _{dic}	19.2 ± 3.8	26.1 ± 8.3	$3.3 \pm 3.1 \cdot 10^{-4}$	0.763
	NQO1 _{apo}	22.0 ± 5.0	37.8 ± 11.7	$3.4 \pm 2.9 \cdot 10^{-4}$	0.791
93-95	NQO1 _{holo}	22.2 ± 5.0	34.2 ± 11.1	$3.6 \pm 3.4 \cdot 10^{-4}$	0.764
	NQO1 _{dic}	24.5 ± 4.8	34.0 ± 11.7	$3.2 \pm 3.0 \cdot 10^{-4}$	0.764
	NQO1 _{apo}	14.0 ± 2.8	22.0 ± 6.6	$3.2 \pm 2.7 \cdot 10^{-4}$	0.803
96	NQO1 _{holo}	14.2 ± 2.8	20.4 ± 7.1	$3.0 \pm 2.8 \cdot 10^{-4}$	0.772
	NQO1 _{dic}	15.3 ± 2.7	19.9 ± 7.1	$2.9 \pm 2.8 \cdot 10^{-4}$	0.770
	NQO1 _{apo}		SLNE		
97	NQO1 _{holo}		SLNE		
	NQO1 _{dic}		SLNE		
98-101	NQO1 _{apo}		SLNE		

	NQO1 _{holo}		SLNE		
	NQO1 _{dic}		SLNE		
102	NQO1 _{apo}		SLNE		
	NQO1 _{holo}		SLNE		
	NQO1 _{dic}		SLNE		
103-106	NQO1 _{apo}	18.9±2.0	58.3±2.3	4.5±0.5·10 ⁻³	0.994
	NQO1 _{holo}	-3.3±1.1	35.0±1.4	2.0±0.3 ·10 ⁻³	0.994
	NQO1 _{dic}		SLNE		
107	NQO1 _{apo}	13.8±2.0	54.7±2.3	4.4±0.5 ·10 ⁻³	0.994
	NQO1 _{holo}	-2.6±0.9	31.8±1.2	1.6±0.2 ·10 ⁻³	0.995
	NQO1 _{dic}		SLNE		
108-109	NQO1 _{apo}	12.2±3.9	42.8±4.6	3.6±1.2·10 ⁻³	0.958
	NQO1 _{holo}	-1.4±0.9	29.3±1.4	9.7±1.5·10 ⁻⁴	0.991
	NQO1 _{dic}		SLNE		
110-113	NQO1 _{apo}	1.8±5.3	45.4±6.2	4.1±1.6·10 ⁻³	0.934
	NQO1 _{holo}	-1.1±1.1	25.9±1.9	6.4±1.5·10 ⁻³	0.980
	NQO1 _{dic}		SLNE		
114-115	NQO1 _{apo}		SLNE		
	NQO1 _{holo}		SLNE		
	NQO1 _{dic}		SLNE		
116-119	NQO1 _{apo}		SLNE		
	NQO1 _{holo}		SLNE		
	NQO1 _{dic}		SLNE		
120-121	NQO1 _{apo}	17.2±3.9	24.4±4.7	3.2±1.9·10 ⁻³	0.876
	NQO1 _{holo}	16.1±1.4	27.2±2.5	6.3±1.8·10 ⁻⁴	0.972
	NQO1 _{dic}		SLNE		
122-124	NQO1 _{apo}	41.2±6.6	43.1±7.0	9.8±4.5·10 ⁻³	0.919
	NQO1 _{holo}	49.3±3.5	36.4±4.4	2.2±0.9·10 ⁻³	0.946
	NQO1 _{dic}		SLNE		

125	NQO1 _{apo}	38.7±8.9	50.2±8.8	3.2±1.1·10 ⁻²	0.958
	NQO1 _{holo}	65.2±2.4	26.7±2.8	4.1±1.2·10 ⁻³	0.961
	NQO1 _{dic}			SLNE	
126	NQO1 _{apo}	57.6±3.4	35.3±3.4	4.0±0.7·10 ⁻²	0.988
	NQO1 _{holo}	84.1±1.0	10.3±1.1	9.6±2.8·10 ⁻³	0.965
	NQO1 _{dic}	31.4±0.7	41.3±7.3	1.6±0.4·10 ⁻⁴	0.991
127	NQO1 _{apo}	63.8±3.3	29.4±3.3	3.8±0.7·10 ⁻²	0.984
	NQO1 _{holo}	86.7±0.7	8.0±0.8	7.4±2.0·10 ⁻²	0.967
	NQO1 _{dic}	33.9±0.5	45.3±6.0	1.1±0.3·10 ⁻⁴	0.995
128	NQO1 _{apo}	67.7±2.3	26.0±2.3	3.0±0.5·10 ⁻²	0.988
	NQO1 _{holo}	84.3±0.8	10.0±0.8	1.0±0.2·10 ⁻²	0.977
	NQO1 _{dic}	43.4±2.4	37.2±6.5	2.8±1.4·10 ⁻⁴	0.934
129	NQO1 _{apo}	62.1±2.3	32.6±2.3	2.5±0.4·10 ⁻²	0.992
	NQO1 _{holo}	76.5±1.2	18.8±1.2	1.4±0.2·10 ⁻²	0.989
	NQO1 _{dic}	36.6±5.8	36.2±6.9	3.5±2.0·10 ⁻³	0.879
130	NQO1 _{apo}	57.5±2.2	38.2±2.2	2.3±0.3·10 ⁻²	0.994
	NQO1 _{holo}	66.9±1.8	29.0±1.8	1.8±0.3·10 ⁻²	0.991
	NQO1 _{dic}	34.2±4.7	47.9±5.3	5.7±1.7·10 ⁻³	0.957
131	NQO1 _{apo}	46.8±2.4	49.4±2.4	2.3±0.3·10 ⁻²	0.996
	NQO1 _{holo}	53.5±2.6	42.6±2.6	2.2±0.3·10 ⁻²	0.993
	NQO1 _{dic}	29.2±2.2	60.7±2.3	7.8±0.8·10 ⁻³	0.995
132	NQO1 _{apo}	37.4±4.1	51.0±4.2	1.5±0.3·10 ⁻²	0.982
	NQO1 _{holo}	42.2±3.8	48.5±3.9	1.1±0.3·10 ⁻²	0.979
	NQO1 _{dic}	21.3±0.6	62.2±0.6	8.9±0.3·10 ⁻³	0.999
133	NQO1 _{apo}	18.0±2.2	48.0±4.5	4.3±1.2·10 ⁻⁴	0.973
	NQO1 _{holo}	11.6±1.1	61.4±1.7	7.9±0.7·10 ⁻⁴	0.997
	NQO1 _{dic}	10.5±0.6	17.2±0.8	3.0±0.4·10 ⁻³	0.994
134-141	NQO1 _{apo}	18.6±1.8	46.7±3.9	3.7±0.9·10 ⁻⁴	0.980
	NQO1 _{holo}	11.8±1.0	59.6±1.7	7.0±0.6·10 ⁻⁴	0.997

	NQO1 _{dic}	11.6±0.5	11.7±0.6	2.9±0.5·10 ⁻³	0.991
142-145	NQO1 _{apo}	5.1±0.2	2.5±0.3	5.7±1.6 ·10 ⁻³	0.961
	NQO1 _{holo}	3.6±0.2	3.1±0.2	4.6±0.9 ·10 ⁻³	0.981
	NQO1 _{dic}	2.6±0.3	2.7±0.4	3.4±1.4 ·10 ⁻³	0.934
	NQO1 _{apo}	22.6±0.6	9.3±0.6	3.6±0.7·10 ⁻³	0.982
146-148	NQO1 _{holo}	15.5±0.4	12.0±0.5	4.1±0.4·10 ⁻³	0.993
	NQO1 _{dic}	10.8±1.0	10.6±1.2	2.8±1.0·10 ⁻³	0.952
	NQO1 _{apo}	56.9±0.6	19.1±0.6	6.3±0.6·10 ⁻³	0.998
149-155	NQO1 _{holo}	44.8±1.3	27.4±1.5	5.2±0.8·10 ⁻³	0.989
	NQO1 _{dic}	31.5±3.1	31.5±3.7	2.7±1.0·10 ⁻³	0.948
	NQO1 _{apo}	44.0±1.1	19.2±1.3	3.6±0.7·10 ⁻³	0.982
156	NQO1 _{holo}	33.2±1.2	24.1±1.4	3.9±0.7·10 ⁻³	0.987
	NQO1 _{dic}	24.5±2.3	26.5±2.8	2.3±0.8·10 ⁻³	0.959
	NQO1 _{apo}	17.3±0.6	21.7±1.0	9.3±1.4·10 ⁻⁴	0.992
157-164	NQO1 _{holo}	6.6±1.1	23.5±1.6	1.2±0.3·10 ⁻³	0.982
	NQO1 _{dic}	5.9±0.7	20.5±1.0	1.4±0.2·10 ⁻³	0.991
	NQO1 _{apo}	12.5±0.8	23.2±1.3	7.4±1.3·10 ⁻⁴	0.989
165	NQO1 _{holo}	1.5±1.3	26.3±2.2	6.7±1.8·10 ⁻⁴	0.974
	NQO1 _{dic}	0.8±0.4	20.0±0.5	1.2±0.1·10 ⁻³	0.998
	NQO1 _{apo}		SLNE		
166	NQO1 _{holo}		SLNE		
	NQO1 _{dic}		SLNE		
	NQO1 _{apo}		SLNE		
167	NQO1 _{holo}		SLNE		
	NQO1 _{dic}		SLNE		
	NQO1 _{apo}		SLNE		
168-173	NQO1 _{holo}		SLNE		
	NQO1 _{dic}		SLNE		
	NQO1 _{apo}		SLNE		
174-175	NQO1 _{apo}		SLNE		

	NQO1 _{holo}		SLNE		
	NQO1 _{dic}		SLNE		
176-177	NQO1 _{apo}		SLNE		
	NQO1 _{holo}		SLNE		
	NQO1 _{dic}		SLNE		
178	NQO1 _{apo}		SLNE		
	NQO1 _{holo}		SLNE		
	NQO1 _{dic}		SLNE		
179-181	NQO1 _{apo}		SLNE		
	NQO1 _{holo}		SLNE		
	NQO1 _{dic}		SLNE		
182	NQO1 _{apo}	0.6±0.4	8.8±0.5	3.2±0.5 ·10 ⁻³	0.990
	NQO1 _{holo}	-0.3±0.2	9.1±0.2	5.7±0.3 ·10 ⁻³	0.999
	NQO1 _{dic}	-0.5±0.2	9.1±0.2	4.2±0.3 ·10 ⁻³	0.998
183-185	NQO1 _{apo}	1.4±0.6	15.2±0.7	3.4±0.5 ·10 ⁻³	0.992
	NQO1 _{holo}	-0.4±0.2	16.0±0.3	5.8±0.3 ·10 ⁻³	0.999
	NQO1 _{dic}	-0.7±0.3	16.0±0.3	4.4±0.2 ·10 ⁻³	0.999
186-189	NQO1 _{apo}	1.9±0.7	21.7±0.9	3.6±0.4 ·10 ⁻³	0.994
	NQO1 _{holo}	-0.5±0.3	22.9±0.4	5.9±0.3 ·10 ⁻³	0.999
	NQO1 _{dic}	-0.9±0.7	22.9±0.5	4.4±0.2 ·10 ⁻³	0.998
190	NQO1 _{apo}	13.9±0.9	21.4±1.1	4.0±0.6 ·10 ⁻³	0.991
	NQO1 _{holo}	7.5±0.3	25.5±0.3	5.4±0.2 ·10 ⁻³	0.999
	NQO1 _{dic}	7.5±0.2	24.9±0.2	4.3±0.1 ·10 ⁻³	0.999
191	NQO1 _{apo}	42.4±1.9	20.6±2.1	7.8±2.2 ·10 ⁻³	0.965
	NQO1 _{holo}	26.3±0.5	35.9±0.5	4.5±0.2 ·10 ⁻³	0.999
	NQO1 _{dic}	27.0±0.8	34.5±0.9	3.8±0.3 ·10 ⁻³	0.997
192-201	NQO1 _{apo}	63.5±5.1	25.7±5.1	4.6±1.4 ·10 ⁻²	0.955
	NQO1 _{holo}	51.3±1.2	38.6±1.4	3.9±0.4 ·10 ⁻³	0.995
	NQO1 _{dic}	52.1±1.0	37.9±1.2	4.1±0.4 ·10 ⁻³	0.997

202-203	NQO1 _{apo}	32.4±3.0	60.3±3.4	5.7±0.9 ·10 ⁻³	0.988
	NQO1 _{holo}	21.4±3.4	59.5±6.4	5.2±1.7 ·10 ⁻⁴	0.962
	NQO1 _{dic}	22.4±3.9	63.5±7.1	5.5±1.9 ·10 ⁻⁴	0.958
204-205	NQO1 _{apo}	5.3±3.3	53.5±4.0	3.4±0.8 ·10 ⁻³	0.979
	NQO1 _{holo}	0.4±0.9	46.1±2.6	2.5±0.4 ·10 ⁻⁴	0.994
	NQO1 _{dic}	1.0±1.2	49.7±3.1	2.9±0.5 ·10 ⁻⁴	0.991
206-211	NQO1 _{apo}	-0.2±0.2	26.9±0.6	2.2±0.1 ·10 ⁻⁴	0.999
	NQO1 _{holo}	-0.1±0.2	3.3±0.6	2.3±1.0 ·10 ⁻⁴	0.955
	NQO1 _{dic}	-0.2±0.2	5.0±0.5	3.4±1.0 ·10 ⁻⁴	0.973
212	NQO1 _{apo}	18.3±4.3	44.8±6.0	1.2±0.6 ·10 ⁻³	0.933
	NQO1 _{holo}	16.0±4.8	43.6±5.8	2.4±1.1 ·10 ⁻³	0.935
	NQO1 _{dic}	14.8±4.9	45.7±5.9	2.5±1.1 ·10 ⁻³	0.939
213-214	NQO1 _{apo}	22.6±5.4	57.5±7.3	1.4±0.6 ·10 ⁻³	0.939
	NQO1 _{holo}	21.2±5.7	60.5±7.4	1.7±0.7 ·10 ⁻³	0.944
	NQO1 _{dic}	19.1±6.0	63±7.5	1.9±0.8 ·10 ⁻³	0.946
215-216	NQO1 _{apo}	24.2±4.9	53.5±6.8	1.3±0.6 ·10 ⁻³	0.940
	NQO1 _{holo}	23.2±5.1	56.6±6.8	1.5±0.6 ·10 ⁻³	0.946
	NQO1 _{dic}	21.4±5.3	59.2±6.9	1.7±0.7 ·10 ⁻³	0.948
217-218	NQO1 _{apo}	25.2±3.5	49.0±5.3	9.6±3.4 ·10 ⁻⁴	0.957
	NQO1 _{holo}	24.7±3.6	52.2±5.2	1.1±0.4 ·10 ⁻³	0.962
	NQO1 _{dic}	23.5±3.7	54.6±5.3	1.1±0.4 ·10 ⁻³	0.964
219	NQO1 _{apo}	22.9±2.1	42.6±3.8	5.6±1.6 ·10 ⁻⁴	0.973
	NQO1 _{holo}	22.2±2.0	44.6±3.6	5.6±1.4 ·10 ⁻⁴	0.978
	NQO1 _{dic}	21.5±2.1	46.0±3.6	6.3±1.6 ·10 ⁻⁴	0.978
220-221	NQO1 _{apo}	21.2±1.7	41.4±3.3	4.9±1.2 ·10 ⁻⁴	0.979
	NQO1 _{holo}	20.1±4.5	43.5±2.9	4.9±1.0 ·10 ⁻⁴	0.985
	NQO1 _{dic}	19.5±1.6	44.8±3.0	5.4±1.1 ·10 ⁻⁴	0.985
222	NQO1 _{apo}	17.9±1.8	43.3±3.4	5.4±1.3 ·10 ⁻⁴	0.980
	NQO1 _{holo}	14.7±1.7	45.6±3.2	5.4±1.1 ·10 ⁻⁴	0.984

	NQO1 _{dic}	13.6±1.7	46.2±2.9	6.1±1.2 ·10 ⁻⁴	0.986
223-228	NQO1 _{apo}	33.8±2.3	32.9±2.7	3.8±0.9 ·10 ⁻³	0.975
	NQO1 _{holo}	25.9±1.8	39.0±2.2	3.8±0.6 ·10 ⁻³	0.989
	NQO1 _{dic}	23.0±1.3	41.1±1.5	3.4±0.4 ·10 ⁻³	0.995
229-231	NQO1 _{apo}	47.2±4.5	45.5±4.4	5.7±0.8 ·10 ⁻²	0.991
	NQO1 _{holo}	49.7±5.6	42.5±5.5	5.7±1.0 ·10 ⁻²	0.984
	NQO1 _{dic}	41.2±0.6	51.0±0.6	1.7±0.4 ·10 ⁻²	0.999
232	NQO1 _{apo}	54.6±6.6	35.2±6.6	3.0±1.1 ·10 ⁻²	0.950
	NQO1 _{holo}	62.5±4.2	28.8±4.2	1.4±0.6 ·10 ⁻²	0.943
	NQO1 _{dic}	40.5±5.1	47.5±5.2	1.2±0.4 ·10 ⁻²	0.964
233-236	NQO1 _{apo}	51.1±3.1	38.0±3.5	6.6±1.7 ·10 ⁻³	0.970
	NQO1 _{holo}	49.8±2.8	41.4±3.1	6.3±1.3 ·10 ⁻³	0.979
	NQO1 _{dic}	33.4±6.3	51.5±7.2	4.8±1.9 ·10 ⁻³	0.995
237	NQO1 _{apo}	44.4±2.9	44.2±3.2	5.8±1.2 ·10 ⁻³	0.980
	NQO1 _{holo}	42.2±2.6	48.6±2.9	5.8±1.0 ·10 ⁻³	0.987
	NQO1 _{dic}	28.4±6.2	55.7±7.3	3.6±1.4 ·10 ⁻³	0.938
238	NQO1 _{apo}	39.3±2.6	48.4±3.1	3.7±0.7 ·10 ⁻³	0.984
	NQO1 _{holo}	36.2±2.6	55.2±3.0	3.9±0.6 ·10 ⁻³	0.989
	NQO1 _{dic}	27.2±6.0	55.6±7.8	1.7±0.8 ·10 ⁻³	0.927
239-240	NQO1 _{apo}	41.1±2.0	47.7±2.3	6.2±0.8 ·10 ⁻³	0.992
	NQO1 _{holo}	34.7±1.7	55.6±1.9	6.4±0.6 ·10 ⁻³	0.996
	NQO1 _{dic}	31.8±3.6	53.4±4.2	5.0±1.0 ·10 ⁻³	0.978
241	NQO1 _{apo}	44.0±2.3	44.8±2.4	1.0±0.2 ·10 ⁻²	0.991
	NQO1 _{holo}	38.7±1.4	50.5±1.4	1.0±0.1 ·10 ⁻²	0.997
	NQO1 _{dic}	38.1±0.7	51.1±0.8	8.4±0.4 ·10 ⁻³	0.999
242	NQO1 _{apo}	41.9±3.2	46.5±3.2	1.6±0.3 ·10 ⁻²	0.988
	NQO1 _{holo}	37.5±2.8	51.0±2.8	1.4±0.2 ·10 ⁻²	0.992
	NQO1 _{dic}	36.7±2.1	51.6±2.2	1.2±0.1 ·10 ⁻²	0.995
243-244	NQO1 _{apo}	37.7±4.2	49.6±4.2	2.0±0.4 ·10 ⁻²	0.985

	NQO1 _{holo}	34.1±3.6	53.7±3.6	1.6±0.3 ·10 ⁻²	0.989
	NQO1 _{dic}	32.5±3.0	54.7±3.0	1.5±0.2 ·10 ⁻²	0.996
245-248	NQO1 _{apo}	31.1±4.9	55.8±4.8	2.8±0.5 ·10 ⁻²	0.988
	NQO1 _{holo}	26.7±4.9	59.5±4.8	2.4±0.4 ·10 ⁻²	0.988
	NQO1 _{dic}	26.4±4.3	60.2±4.2	2.1±0.4 ·10 ⁻²	0.990
249-251	NQO1 _{apo}	41.2±4.1	28.8±4.5	6.4±2.8 ·10 ⁻³	0.917
	NQO1 _{holo}	34.5±4.8	34.4±5.4	6.1±2.7 ·10 ⁻³	0.916
	NQO1 _{dic}	32.6±5.3	33.7±5.8	7.7±3.7 ·10 ⁻³	0.905
252-254	NQO1 _{apo}	34.8±3.1	30.2±4.9	8.5±4.5 ·10 ⁻⁴	0.910
	NQO1 _{holo}	27.7±4.4	35.7±6.7	9.0±5.6 ·10 ⁻⁴	0.882
	NQO1 _{dic}	27.4±4.7	34.1±7.9	6.8±5.1 ·10 ⁻⁴	0.837
255	NQO1 _{apo}	28.9±1.8	41.0±2.2	2.4±0.4 ·10 ⁻³	0.989
	NQO1 _{holo}	22.5±1.8	48.3±2.4	1.6±0.3 ·10 ⁻³	0.990
	NQO1 _{dic}	23.3±1.9	48.0±2.3	2.6±0.4 ·10 ⁻³	0.991
256-260	NQO1 _{apo}	29.2±1.7	42.1±2.1	2.4±0.4 ·10 ⁻³	0.991
	NQO1 _{holo}	21.9±1.9	50.3±2.5	1.6±0.3 ·10 ⁻³	0.990
	NQO1 _{dic}	22.5±1.9	50.8±2.3	2.7±0.4 ·10 ⁻³	0.992
261	NQO1 _{apo}	29.3±1.4	45.0±1.7	2.7±0.3 ·10 ⁻³	0.994
	NQO1 _{holo}	21.6±1.7	52.2±2.2	1.7±0.2 ·10 ⁻³	0.993
	NQO1 _{dic}	22.0±1.6	52.6±1.9	3.0±0.3 ·10 ⁻³	0.995
262	NQO1 _{apo}	30.2±1.3	44.8±1.6	2.7±0.3 ·10 ⁻³	0.995
	NQO1 _{holo}	21.9±1.6	51.9±2.1	1.8±0.2 ·10 ⁻³	0.993
	NQO1 _{dic}	22.3±1.4	52.3±1.7	3.1±0.3 ·10 ⁻³	0.996
263	NQO1 _{apo}	31.3±1.2	46.6±1.5	2.9±0.3 ·10 ⁻³	0.996
	NQO1 _{holo}	23.5±1.6	53.3±2.0	1.8±0.2 ·10 ⁻³	0.993
	NQO1 _{dic}	23.5±1.3	54.2±1.5	3.2±0.3 ·10 ⁻³	0.997
264-271	NQO1 _{apo}	32.1±1.1	47.9±1.3	3.1±0.3 ·10 ⁻³	0.997
	NQO1 _{holo}	23.8±1.5	55.3±1.9	1.9±0.2 ·10 ⁻³	0.995
	NQO1 _{dic}	23.9±1.3	56.2±1.6	3.4±0.3 ·10 ⁻³	0.997

Table S2. Kinetic parameters for fitting of HDX kinetics to a three-parameter exponential function for 39 experimental peptides covering almost the entire NQO1 sequence. SLNE indicates slow, little or no exchange. PF indicates poor fitting.

Peptide	NQO1 protein	Aburst (%D)	A _{slow} (%D)	k _{slow} (s ⁻¹)	R ²
1-7	NQO1 _{apo}	22.3±2.7	15.8±2.8	1.3±0.6·10 ⁻²	0.914
	NQO1 _{holo}	23.0±2.8	15.0±2.8	1.2±0.6·10 ⁻²	0.898
	NQO1 _{dic}	23.5±2.6	16.1±2.7	1.0±0.5·10 ⁻²	0.912
7-10	NQO1 _{apo}		SLNE		
	NQO1 _{holo}		SLNE		
	NQO1 _{dic}		SLNE		
11-19	NQO1 _{apo}	69.1±1.7	17.4±1.7	1.2±0.3·10 ⁻²	0.971
	NQO1 _{holo}	32.8±0.8	37.4±1.1	1.4±0.1·10 ⁻³	0.997
	NQO1 _{dic}	31.2±0.2	6.0±0.2	3.4±0.4·10 ⁻³	0.995
20-23	NQO1 _{apo}		SLNE		
	NQO1 _{holo}		SLNE		
	NQO1 _{dic}		SLNE		
24-33	NQO1 _{apo}	-1.3±0.6	19.5±0.9	8.9±1.4·10 ⁻⁴	0.992
	NQO1 _{holo}	-1.6±0.8	20.3±1.2	9.0±1.8·10 ⁻⁴	0.987
	NQO1 _{dic}	-1.5±0.6	19.8±0.9	8.8±1.3·10 ⁻⁴	0.993
34-39	NQO1 _{apo}	11.0±1.1	34.1±1.1	1.4±0.1·10 ⁻²	0.997
	NQO1 _{holo}	10.9±0.9	34.7±0.9	1.4±0.1·10 ⁻²	0.998
	NQO1 _{dic}	10.4±0.3	35.1±0.3	1.3±0.1·10 ⁻²	1.000
42-45	NQO1 _{apo}	1.6±4.2	77.8±6.7	7.7±2.2·10 ⁻⁴	0.973
	NQO1 _{holo}	0.6±2.6	74.4±4.7	5.4±1.1·10 ⁻⁴	0.986
	NQO1 _{dic}	2.0±2.3	72.4±4.2	5.7±1.0·10 ⁻⁴	0.988
46-54	NQO1 _{apo}	41.0±3.2	40.2±3.9	2.3±0.7·10 ⁻³	0.964
	NQO1 _{holo}	33.1±3.3	39.2±5.2	7.9±3.4·10 ⁻⁴	0.939
	NQO1 _{dic}	30.1±2.3	25.7±3.9	6.5±3.1·10 ⁻⁴	0.923
55-59	NQO1 _{apo}	83.6±2.6	7.1±2.6	3.4±2.3·10 ⁻²	0.845

	NQO1 _{holo}	58.2±0.7	32.9±0.7	1.0±0.1·10 ⁻²	0.998
	NQO1 _{dic}	58.4±0.5	32.1±0.7	7.2±0.5·10 ⁻⁴	0.998
60-65	NQO1 _{apo}	51.0±42.8	41.2±42.5	1.2±1.0·10 ⁻¹	0.892
	NQO1 _{holo}	38.1±4.1	53.0±4.1	2.8±0.5·10 ⁻²	0.991
	NQO1 _{dic}	32.0±2.3	59.6±2.3	1.4±0.2·10 ⁻²	0.996
66-73	NQO1 _{apo}	52.3±5.3	36.6±5.2	6.9±1.2·10 ⁻²	0.985
	NQO1 _{holo}	26.9±1.5	63.5±1.5	1.3±0.1·10 ⁻²	0.998
	NQO1 _{dic}	26.3±3.8	59.4±6.2	7.3±2.5·10 ⁻⁴	0.961
74-87	NQO1 _{apo}	36.9±4.6	39.7±5.5	3.3±1.4·10 ⁻³	0.931
	NQO1 _{holo}	10.7±5.1	60.9±5.6	7.0±1.8·10 ⁻³	0.970
	NQO1 _{dic}	9.8±2.8	49.4±4.4	8.1±2.4·10 ⁻⁴	0.971
88-92	NQO1 _{apo}		SLNE		
	NQO1 _{holo}		SLNE		
	NQO1 _{dic}		SLNE		
92-96	NQO1 _{apo}	22.5±4.1	33.2±9.6	3.3±2.7·10 ⁻⁴	0.814
	NQO1 _{holo}	22.9±4.1	30.6±9.9	3.2±2.9·10 ⁻⁴	0.783
	NQO1 _{dic}	24.5±4.0	29.6±9.0	3.5±3.1·10 ⁻⁴	0.790
96-102	NQO1 _{apo}		SLNE		
	NQO1 _{holo}		SLNE		
	NQO1 _{dic}		SLNE		
103-107	NQO1 _{apo}	19.1±3.8	62.5±4.5	4.1±0.8·10 ⁻³	0.981
	NQO1 _{holo}	-6.8±2.3	35.5±2.8	2.4±0.6·10 ⁻³	0.977
	NQO1 _{dic}		SLNE		
108-113	NQO1 _{apo}	1.9±4.8	44.9±5.7	3.8±1.4·10 ⁻³	0.943
	NQO1 _{holo}	-1.2±1.1	26.4±2.0	5.9±1.4·10 ⁻⁴	0.981
	NQO1 _{dic}		SLNE		
114-119	NQO1 _{apo}	---	---	---	---
	NQO1 _{holo}	---	---	---	---
	NQO1 _{dic}	---	---	---	---

120-124	NQO1 _{apo}	32.0 ± 5.2	46.1 ± 8.2	$8.4 \pm 4.9 \cdot 10^{-4}$	0.893
	NQO1 _{holo}	23.2 ± 2.1	52.8 ± 4.2	$4.4 \pm 1.0 \cdot 10^{-4}$	0.980
	NQO1 _{dic}	SLNE			
125-129	NQO1 _{apo}	54.0 ± 3.2	37.1 ± 3.2	$4.5 \pm 0.6 \cdot 10^{-2}$	0.991
	NQO1 _{holo}	PF			
	NQO1 _{dic}	PF			
129-132	NQO1 _{apo}	36.6 ± 2.9	62.3 ± 2.9	$2.0 \pm 0.2 \cdot 10^{-2}$	0.995
	NQO1 _{holo}	40.9 ± 2.6	58.9 ± 2.6	$2.0 \pm 0.2 \cdot 10^{-2}$	0.996
	NQO1 _{dic}	19.7 ± 0.5	77.7 ± 0.5	$9.2 \pm 0.2 \cdot 10^{-3}$	1.000
133-141	NQO1 _{apo}	16.7 ± 2.0	47.8 ± 4.2	$3.9 \pm 1.0 \cdot 10^{-4}$	0.977
	NQO1 _{holo}	10.4 ± 0.9	61.5 ± 1.5	$8.0 \pm 0.6 \cdot 10^{-4}$	0.998
	NQO1 _{dic}	9.6 ± 0.7	15.2 ± 0.9	$2.6 \pm 0.5 \cdot 10^{-3}$	0.987
142-145	NQO1 _{apo}	SLNE			
	NQO1 _{holo}	SLNE			
	NQO1 _{dic}	SLNE			
146-156	NQO1 _{apo}	47.8 ± 1.2	20.6 ± 1.4	$3.3 \pm 0.7 \cdot 10^{-3}$	0.982
	NQO1 _{holo}	33.2 ± 0.9	25.7 ± 1.1	$4.1 \pm 0.5 \cdot 10^{-3}$	0.993
	NQO1 _{dic}	23.3 ± 2.1	22.8 ± 2.6	$2.9 \pm 1.0 \cdot 10^{-3}$	0.954
157-165	NQO1 _{apo}	12.5 ± 0.8	23.2 ± 1.3	$7.4 \pm 1.3 \cdot 10^{-4}$	0.989
	NQO1 _{holo}	1.5 ± 1.3	26.2 ± 2.2	$6.7 \pm 1.8 \cdot 10^{-4}$	0.975
	NQO1 _{dic}	0.8 ± 0.4	20.0 ± 0.5	$1.2 \pm 0.1 \cdot 10^{-3}$	0.998
166-173	NQO1 _{apo}	SLNE			
	NQO1 _{holo}	SLNE			
	NQO1 _{dic}	SLNE			
174-181	NQO1 _{apo}	SLNE			
	NQO1 _{holo}	SLNE			
	NQO1 _{dic}	SLNE			
182-189	NQO1 _{apo}	-0.2 ± 0.2	19.2 ± 0.3	$2.9 \pm 0.1 \cdot 10^{-3}$	0.999

	NQO1 _{holo}	-1.1±0.4	19.8±0.5	5.4±0.4·10 ⁻³	0.998
	NQO1 _{dic}	-1.8±0.6	19.9±0.7	4.1±0.4·10 ⁻³	0.996
190-201	NQO1 _{apo}	74.6±1.9	16.1±2.1	5.7±2.1·10 ⁻³	0.939
	NQO1 _{holo}	49.8±1.3	35.4±1.5	3.4±0.4·10 ⁻³	0.993
	NQO1 _{dic}	51.2±1.7	31.1±2.0	3.2±0.6·10 ⁻³	0.984
202-205	NQO1 _{apo}	8.6±2.5	86.0±2.9	4.8±0.5·10 ⁻³	0.996
	NQO1 _{holo}	0.2±2.1	82.7±6.1	2.7±0.5·10 ⁻⁴	0.989
	NQO1 _{dic}	1.3±2.9	88.2±7.6	2.9±0.7·10 ⁻⁴	0.982
206-211	NQO1 _{apo}	-1.3±0.3	25.9±0.8	2.4±0.2·10 ⁻⁴	0.998
	NQO1 _{holo}		SLNE		
	NQO1 _{dic}		SLNE		
212-218	NQO1 _{apo}	17.2±5.5	63.0±7.3	1.6±0.6·10 ⁻³	0.949
	NQO1 _{holo}	17.1±5.9	66.7±7.6	1.8±0.7·10 ⁻³	0.950
	NQO1 _{dic}	15.6±6.1	69.5±7.8	1.8±0.7·10 ⁻³	0.952
219-222	NQO1 _{apo}	21.8±0.6	45.4±1.4	3.0±0.3·10 ⁻⁴	0.998
	NQO1 _{holo}	-1.0±1.0	49.3±3.1	2.4±0.4·10 ⁻⁴	0.993
	NQO1 _{dic}	-0.6±0.7	48.0±2.0	2.8±0.3·10 ⁻⁴	0.996
223-228	NQO1 _{apo}	37.1±1.5	30.2±1.6	6.4±1.0·10 ⁻³	0.989
	NQO1 _{holo}	29.9±1.2	34.9±1.4	5.4±0.6·10 ⁻³	0.994
	NQO1 _{dic}	26.6±0.8	37.6±0.9	4.8±0.3·10 ⁻³	0.998
229-232	NQO1 _{apo}	47.2±4.5	45.5±4.5	5.7±0.8·10 ⁻²	0.991
	NQO1 _{holo}	49.7±5.9	42.5±5.5	5.7±1.0·10 ⁻²	0.983
	NQO1 _{dic}	41.2±0.7	51.0±0.6	1.7±0.1·10 ⁻²	1.000
233-238	NQO1 _{apo}	35.9±3.1	50.1±3.7	4.1±0.9·10 ⁻³	0.980
	NQO1 _{holo}	35.9±3.2	54.5±3.8	4.0±0.8·10 ⁻³	0.982
	NQO1 _{dic}	20.8±7.7	58.0±9.3	2.7±1.4·10 ⁻³	0.910
239-248	NQO1 _{apo}	40.9±3.0	48.6±3.0	1.4±0.2·10 ⁻²	0.989
	NQO1 _{holo}	34.0±3.1	54.8±3.1	1.5±0.2·10 ⁻²	0.991
	NQO1 _{dic}	34.7±2.7	53.9±2.7	1.2±0.2·10 ⁻²	0.992

249-254	NQO1 _{apo}	34.8±3.1	30.2±4.9	8.5±4.5·10 ⁻⁴	0.911
	NQO1 _{holo}	27.7±4.4	35.7±6.7	9.0±5.6·10 ⁻⁴	0.882
	NQO1 _{dic}	27.4±4.7	34.1±7.9	6.8±5.1·10 ⁻⁴	0.837
255-271	NQO1 _{apo}	28.9±1.8	41.0±2.2	2.4±0.4·10 ⁻³	0.989
	NQO1 _{holo}	22.5±1.8	48.3±2.4	1.6±0.3·10 ⁻³	0.990
	NQO1 _{dic}	23.3±1.9	48.0±2.3	2.6±0.4·10 ⁻³	0.991

Supplementary references

1. Medina-Carmona, E.; Neira, J.L.; Salido, E.; Fuchs, J.E.; Palomino-Morales, R.; Timson, D.J.; Pey, A.L. Site-to-site interdomain communication may mediate different loss-of-function mechanisms in a cancer-associated NQO1 polymorphism. *Scientific Reports* **2017**, *7*, 44352.
2. Kavan, D.; Man, P. MSTools-Web based application for visualization and presentation of HXMS data. *Int. J. Mass Spectrom.* **2011**, *302*, 53-58.
3. Faig, M.; Bianchet, M.A.; Talalay, P.; Chen, S.; Winski, S.; Ross, D.; Amzel, L.M. Structures of recombinant human and mouse NAD(P)H:quinone oxidoreductases: species comparison and structural changes with substrate binding and release. *Proc Natl Acad Sci U S A* **2000**, *97*, 3177-3182.
4. Asher, G.; Dym, O.; Tsvetkov, P.; Adler, J.; Shaul, Y. The crystal structure of NAD(P)H quinone oxidoreductase 1 in complex with its potent inhibitor dicoumarol. *Biochemistry* **2006**, *45*, 6372-6378.